FORSCHUNGSZENTRUM
ROSSENDORF e.V.

FZR

FZR-119
December 1995
Preprint

E. Persson, M. Müller and I. Rotter

Resonance phenomena near thresholds

Forschungszentrum Rossendorf e.V.
Postfach 51 01 19 · D-01314 Dresden
Bundesrepublik Deutschland

Telefon (0351) 260 3281
Telefax (0351) 260 3700
E-Mail rotter@fz-rossendorf.de

Resonance phenomena near thresholds

E. Persson[1], M. Müller[1], and I. Rotter[1,2]

[1] *Forschungszentrum Rossendorf, Institut für Kern- und Hadronenphysik, D-01314 Dresden, Germany*

[2] *Technische Universität Dresden, Institut für Theoretische Physik, D-01062 Dresden, Germany*

Abstract

The trapping effect is investigated close to the elastic threshold. The nucleus is described as an open quantum mechanical many-body system embedded in the continuum of decay channels. An ensemble of compound nucleus states with both discrete and resonance states is investigated in an energy-dependent formalism. It is shown that the discrete states can trap the resonance ones and also that the discrete states can directly influence the scattering cross section.

1 Introduction

In different theoretical investigations of open many-particle quantum systems it was found that, at a critical value of the level density, a redistribution of the spectroscopic properties takes place [1] – [22]: The transition from low to high level density creates well separated narrow resonances which are enveloped by a few broad ones acting like a dynamical contribution to the potential scattering. As a consequence, some long-lived states exist at high level density together with a few short-lived ones. The corresponding reaction time scales are well separated from each other (*trapping effect*). All these studies are performed far from particle decay thresholds, where the number of short-lived states is equal to the number of open decay channels.

In heavy nuclei, however, the excitation region just above the elastic (first particle decay) threshold is most interesting. Here, the total cross section for neutron scattering shows the picture of well separated resonances although the level density is very high. The widths of these neutron resonances in heavy nuclei are of the order of magnitude of keV or even eV. They interfer with the smooth potential scattering the contribution of which to the total cross section is large.

In the standard description of the neutron resonances, threshold effects are not taken into account [23, 24] although they are lying in the very neighbourhood of the elastic neutron threshold. The neutron resonances are described either as discrete states by means of strongly mixed bound-state wavefunctions or on the basis of the statistical theory of nuclear reactions where no thresholds at all exist. In any case, threshold effects in the wavefunctions and positions of the neutron resonances are neglected.

It is, indeed, suggestive to interprete the neutron resonances as trapped states [7, 12]. It is, however, difficult (or almost impossible) to prove this suggestion by analysing the total cross section. The main reason is, that the cross section is an interference picture to which all resonances contribute and, furthermore, that the neutron resonances are lying in the very neighbourhood of the first neutron decay threshold.

The *cross section* is the result of interferences between narrow resonances and a smooth (almost energy independent) reaction part. The smooth part may arise from both the direct reaction part and the short-lived resonance, which is formed together with the long-lived resonance states at high level density due to the trapping effect. The short-lived resonance may be interpreted as a dynamical part to the potential [9]. It is, therefore, almost impossible to distinguish it in the cross section from the direct reaction part, especially if one takes into account that neither the potential nor the residual interaction is calculated in nuclear physics but is fitted to data.

Furthermore, the *widths* of trapped states lying just above the elastic threshold are small as a result of both the trapping effect and their position in energy. It is again very difficult (or even impossible) to prove whether the widths of the neutron resonances are so extremely small only because of their position in the very neighbourhood of the elastic threshold or whether the interference of the resonances (trapping effect) is needed to explain the small width of the neutron resonances..

In spite of the problems mentioned above we state that the interpretation of the neutron resonances as trapped states is *not* in disagreement with their known properties although they are mostely considered as isolated resonances. In any case, the background is large. The resonance reaction part represents only a small part of the total neutron scattering cross section.

In this paper we study the influence of the lowest particle decay threshold on the trapping effect in order to simulate the real situation of neutron resonances. That means, we investigate an ensemble consisting of discrete *as well as* of resonance states.

The numerical calculations are performed in the framework of the continuum shell model [7, 17] which is, to our knowledge, the only one allowing for a description of the trapping effect near particle decay thresholds. In this model, the widths Γ_R and energies E_R of the resonance states are obtained, by solving the fixpoint equations, from the complex eigenvalues $\tilde{\mathcal{E}}_R = \tilde{E}_R - \frac{i}{2}\,\tilde{\Gamma}_R$ of the effective Hamilton operator H^{eff}_{QQ} which describes the open quantum system. The eigenvalues are energy dependent functions and their energy dependency is needed when calculating the total scattering cross section σ^{tot}. The energy dependence is, however, smooth up to threshold effects in the imaginary parts $\mathrm{Im}(\tilde{\mathcal{E}}_R) = \frac{1}{2}\tilde{\Gamma}_R$. The $\tilde{\Gamma}_R$ vanish below the first particle decay threshold but are different from zero above it.

In Sect. 2 of this paper, the continuum shell model is sketched. The eigenvalues of the effective Hamiltonian H^{eff}_{QQ} are calculated under different conditions as a function of the coupling strength α between the resonance states in the compound nucleus and the continuum of decay channels. The influence of a threshold does not destroy the trapping effect (Sect. 3). It is possible that all the states lying above the threshold (resonances) are trapped while the states with a large spectroscopic factor are discrete. This result corresponds to the fact that the states, the spectroscopic factors of which are large, appear mostly in the lower part of the spectrum [17]. In Sect. 4, the influence of discrete states lying near to the elastic threshold on the scattering cross section is investigated. Conclusions from the results obtained are drawn in the last section.

2 The model

The Hamiltonian of an open quantum system can be written in the following manner [7, 17]

$$H^{eff}_{QQ}(E) \;=\; H_{QQ} + V_{QP}\, G^{(+)}_{P}(E)\, V_{PQ}\;, \tag{1}$$

where $H_{QQ} = H^0_{QQ} + V_{QQ}$ is the Hamiltonian of the corresponding closed system,

$$(H_{QQ} - E^{SM}_R)\,\Phi^{SM}_R = 0\;, \tag{2}$$

V is the residual interaction between two (bound or unbound) particles of the system, $G^{(+)}_P$ is the Green function for the motion of the particle in the continuum of decay channels. The operators Q and P project onto the subspaces of the discrete and continuous states, respectively,

$$Q = \sum_{R=1}^{N} |\Phi^{SM}_R\rangle\,\langle\Phi^{SM}_R| \tag{3}$$

and

$$P = \sum_{c=1}^{\Lambda} \int_{\epsilon_c}^{\infty} dE \, |\xi_E^{c(+)}\rangle \, \langle \xi_E^{c(+)}| \, . \tag{4}$$

The channels c open at the energies $E = \epsilon_c$. The matrix elements of V_{QP} are $\langle \Phi_R^{SM} | V | \xi_E^c \rangle$ and a corresponding expression holds for those of V_{PQ}.

In the continuum shell model, the energy dependence of eigenfunctions $\tilde{\Phi}_R^{(+)}(E)$ and eigenvalues $\tilde{E}_R(E) - \frac{i}{2}\tilde{\Gamma}_R(E)$ of the effective Hamiltonian (1),

$$H_{QQ}^{eff}(E) \, \tilde{\Phi}_R^{(+)}(E) = \left(\tilde{E}_R(E) - \frac{i}{2}\tilde{\Gamma}_R(E)\right) \tilde{\Phi}_R^{(+)}(E) \, , \tag{5}$$

does not show any resonance behaviour due to the cut-off technique used for the single-particle resonances [25]. The eigenvalues depend rather smoothly on the energy E of the system up to threshold effects in the imaginary part $\frac{1}{2}\tilde{\Gamma}_R(E)$. Therefore, the positions E_R and widths Γ_R of the resonance states R can be determined uniquely by solving the fixpoint equations [25]. Due to the weak energy dependence of $\tilde{E}_R(E)$ and $\tilde{\Gamma}_R(E)$ far from thresholds, the energies E_R and widths Γ_R of all resonance states of an ensemble at high level density can be determined to a good approximation from the $\tilde{E}_R(E)$ and $\tilde{\Gamma}_R(E)$ calculated at a certain energy E lying at about the middle of the spectrum [17, 19]. The advantage of such a calculation is that the wavefunctions $\tilde{\Phi}_R(E)$ of all the resonance states are, at the energy E, eigenfunctions of the same Hamilton operator $H_{QQ}^{eff}(E)$.

The effective Hamiltonian H_{QQ}^{eff} is non-hermitean and the following relations hold for it's eigenfunctions $\tilde{\Phi}_R$ [7, 17]

,

$$\langle \tilde{\Phi}_R^* | \tilde{\Phi}_{R'} \rangle = \delta_{RR'} \, , \tag{6}$$

$$\langle \tilde{\Phi}_R | \tilde{\Phi}_R \rangle \geq 1 \, . \tag{7}$$

The trapping effect appears if the second part of the Hamiltonian (1) is important relative to the first part. In such a case, the non-diagonal matrix elements are large with the result that the diagonal matrix elements are essentially different from the eigenvalues of H_{QQ}^{eff}. Also the real eigenfunctions Φ_R^{SM} of H_{QQ} are essentially different from the complex eigenfunctions $\tilde{\Phi}_R$ of H_{QQ}^{eff}. The spectroscopic factors can therefore no longer be calculated from the eigenfunctions of H_{QQ}. At least, H_{QQ} should be replaced by

$$H'_{QQ} \;\; = \;\; H_{QQ} + Re\{V_{QP} G_P^{(+)} V_{PQ}\} \tag{8}$$

according to (1) .

Due to the trapping effect, different time scales exist at high level density and

$$\sum_{R=1}^{N} \tilde{\Gamma}_R \;=\; \sum_{R=1}^{K} \tilde{\Gamma}_R \;+\; \sum_{R=K+1}^{N} \tilde{\Gamma}_R \tag{9}$$

with

$$\sum_{R=1}^{K} \tilde{\Gamma}_R \;\gg\; \sum_{R=K+1}^{N} \tilde{\Gamma}_R \tag{10}$$

where K is the number of *open* decay channels. The relation (10) is a consequence of the fact that in (1) the rank of H_{QQ} is N while that of the second term $H_{QP}G_P^{(+)}H_{PQ}$ is $K < N$.

In this paper, we are interested in the influence of a threshold on the trapping effect. Therefore the most interesting results are at an energy E of the system where only one decay channel is open ($K = 1$). In the one-channel case, the spectroscopic factors of the states are proportional to the $\Gamma_R = \tilde{\Gamma}_R(E = E_R)$.

The S-matrix reads [7]

$$S_{cc'} = e^{2i\delta_c} - 2i\pi\langle\chi_E^{c'(-)}|V|\xi_E^{c(+)}\rangle - i\sum_R \frac{\tilde{\gamma}_{Rc'}^{1/2}\;\tilde{\gamma}_{Rc}^{1/2}}{E - (\tilde{E}_R - \frac{i}{2}\,\tilde{\Gamma}_R)}\,. \tag{11}$$

Here the $\chi_E^{c'(-)}$ are the uncoupled channel wavefunctions. The matrix elements

$$\tilde{\gamma}_{Rc}^{1/2} = (2\pi)^{1/2}\,\langle\tilde{\Phi}_R^{(-)}|V|\xi_E^{c(+)}\rangle \tag{12}$$

are energy dependent complex functions describing the coupling among the resonance states $\tilde{\Phi}_R$ and the channels ξ_E^c. The $\tilde{\gamma}_{Rc}$ are proportional to the partial widths $\tilde{\Gamma}_{Rc} = \tilde{\gamma}_{Rc}/\langle\tilde{\Phi}_R|\tilde{\Phi}_R\rangle$ of the resonance states R with respect to the channels c.

In (11), not only the $\tilde{\gamma}_{Rc}^{1/2}$ are energy dependent functions but also the $\tilde{\Gamma}_R$ and $\tilde{E}_R$. By means of the S-matrix, the cross section can be calculated

$$\sigma = \frac{\hbar^2\pi^2}{2mE}|1 - S|^2\,. \tag{13}$$

In order to investigate the behaviour of the eigenvalues of H_{QQ}^{eff} as a function of the coupling strength between discrete and continuous states, the residual interaction V in the coupling matrix elements $\langle \Phi_R^{SM} | V | \xi_E^c \rangle$ is replaced by $\alpha \cdot V$ and the coupling parameter α is varied. Then, $\alpha = 0$ corresponds to the closed system described by the Hamiltonian H_{QQ} while for $\alpha = 1$ the residual interaction V in H_{QQ} between bound states is equal to the interaction V between discrete and continuous states. The values $\alpha > 1$ describe some density dependence of nuclear forces in a simplified manner.

All calculations in the present paper are performed for an ensemble of 190 resonance states in ^{16}O with $J^\pi = 1^-$ and $2p-2h$ nuclear structure $((1s)^{-1}(1p)^{-1}(2s,1d)^2)$. The residual interaction is of zero-range type with spin exchange term

$$V(\vec{r}_1, \vec{r}_2) = V_0(a + bP_{12}^\sigma)\delta(\vec{r}_1 - \vec{r}_2) \; . \tag{14}$$

The number of open decay channels is $K = 1$, which is either the proton channel $^{15}N_{3/2^-} + p$ or the neutron channel $^{15}O_{3/2^-} + n$. The parameters of the Woods-Saxon potential for neutrons as well as for protons are taken from calculations describing proton scattering on ^{15}N [17, 25]. The Coulomb potential corresponds to a homogeneous charged sphere of radius 3.08 fm and 3.01 fm for O and N respectively. The parameters of the residual interaction V are the same as in [17].

3 The eigenvalue picture

For illustration, the propagation of the complex eigenvalues with growing coupling to the continuum α is shown in Fig. 1.a for an ensemble of 190 resonances with $J^\pi = 1^-$ and only the elastic neutron decay channel is open. The real parts $\tilde{E}_R$ of the complex eigenvalues are drawn on the abscisse, the imaginary parts $\frac{1}{2}\tilde{\Gamma}_R$ on the ordinate. With growing coupling parameter α each eigenvalue is following a certain trajectory.

In the example shown in Fig. 1.a, all states but the one with the largest $\frac{1}{2}\tilde{\Gamma}_R$ are lying at energies larger than $10MeV$ for all α. The energy E_{lab} of the incoming particle is chosen to be $29MeV$, which is approximately in the middle of the whole spectrum and far away from the elastic threshold. In this region the eigenvalues $\tilde{\varepsilon}_R = \tilde{E}_R - \frac{i}{2}\tilde{\Gamma}_R$ of H_{QQ}^{eff} are almost constant as a function of the energy E_{lab}. The $\tilde{\varepsilon}_R(E = 29MeV)$ therefore give the resonance parameters E_R and Γ_R for all the states to a good approximation.

In Fig. 1.b, the imaginary parts $\frac{1}{2}\tilde{\Gamma}_R$ of the complex eigenvalues $\tilde{\varepsilon}_R(E)$ are drawn as a function of the strength parameter α. As it can be seen,

the lifetime of one resonance is getting well separated from the other ones at high coupling strength. The separation starts if the mean overlap of the states reaches a critical value ($\alpha \approx 2$) and one broad resonance state is formed (trapping effect). This broad resonance is lying at about $14MeV$ for small α (see Fig. 1.a) but at much smaller energies for large α.

In the following we want to study the *same* ensemble of 190 states but situated around the elastic threshold. This is done by reducing the shell model energies (eigenvalues of H_{QQ}) of all the states by an energy ΔE^{sm}. This is equivalent to subtracting $\Delta E^{sm} \cdot 1$ from H_{QQ}^{eff}. Thus, if calculating at the same fixed system energy $E = E_{lab}$, it means nothing else than subtracting the same ΔE^{sm} from all $\tilde{E}_R$. This leaves the shape of the eigenvalue picture as a function of the coupling strength α *unchanged* apart from the redefinition of the zero on the abscisse. This is true even if ΔE^{sm} is chosen so large that some of the $\tilde{E}_R$ are negative.

In order to interprete the complex eigenvalue $\tilde{\varepsilon}_R(E)$ of H_{QQ}^{eff} as position E_R and inverse lifetime Γ_R of a certain state, it is necessary to solve the fixpoint equations. That means, one has to calculate $\tilde{\varepsilon}_R(E_R)$ at the energy $E = E_R$ of the resonance for being able to interprete $\tilde{\Gamma}_R(E_R)$ as Γ_R of the state considered. If $\tilde{\Gamma}_R(E)$ shows a strong energy dependency caused e.g. by thresholds, $\tilde{\Gamma}_R(E \neq E_R)$ may be very different from Γ_R. For the elastic threshold, this effect is very large, because as $E_{lab} \to 0$ all $\tilde{\Gamma}_R(E) \to 0$.

In our calculation (Fig. 2) the shift ΔE^{sm} is choosen to be 25 MeV, which makes nearly half of the spectrum situated below the elastic threshold, i.e. nearly half of the spectrum consists of discrete states. The energy of the incident particle is fixed at $E_{lab} = 4MeV$. As in Fig. 1, the coupling between bound and scattering states is increased with the help of the strength parameter α.

In spite of the fact that many states are discrete, all the eigenvalues $\tilde{\varepsilon}_R(E > 0) = \tilde{E}_R(E > 0) - \frac{i}{2}\tilde{\Gamma}_R(E > 0)$ carry an imaginary part $\tilde{\Gamma}_R$ which is different from 0. Moreover, the state with the largest $\tilde{\Gamma}_R$ arises from the set of discrete states. This state causes the trapping and gets large negative $\tilde{E}_R(E > 0)$ in agreement with the results shown in Fig. 1.

In contrast to Fig.1, all the resonances are getting trapped in Fig. 2. No short time scale, in terms of a short-lived *resonance*, is formed. The imaginary part of the states below the elastic threshold which is calculated at $E = E_{lab}$, cannot be interpreted as the inverse lifetime Γ_R of those states and the extraction of the corresponding spectroscopic factors is difficult. Also, the $\tilde{\Gamma}_R(E)$ show strong energy dependence near the elastic threshold.

Therfore it is difficult to draw conclusions from the eigenvalue picture, calculated at a certain fixed energy $E_{lab} > E_R$, for the resonance states in the very neighbourhood of the threshold.

In order to avoid the problems arising from the strong energy dependency of $\tilde{\Gamma}_R(E)$ at $E_{lab} \approx 0$ we did as follows: We created a gap in the level distribution around the region of the elastic threshold by shifting the upper ($E_R > 0$) and the lower ($E_R < 0$) half of the spectrum additionally in the positive and negative direction, respectively. As a result, all states are placed at least a few MeV either below or above the elastic threshold.

The results are plotted in Fig. 3. The real and imaginary parts belonging to the eigenvalues of the states of this ensemble are given for various coupling strengths α as in Figs. 1a and 2. The calculation is performed at $E_{lab} = 4MeV$. With this arrangement the $\tilde{\Gamma}_R(E_{lab})$ of the resonances give a good approximation for the inverse lifetimes of the corresponding states.

The results are as follows: the eigenvalues of the resonance states ($E_R > 0$) propagate for small and intermediate α in a manner similar to the eigenvalues shown in Fig. 1.a (however, the number of resonances is much smaller in Fig. 2 than in Fig. 1.a). A resonance at small energy dominates the decay behaviour of the resonances for intermediary α. At larger α, however, this broad state also starts to get trapped. As a result there are only trapped resonances. No one of the resonances is short-lived at large α.

This calculation proves that discrete states are able to trap *all* resonances in the neighbourhood of the elastic threshold. The influence of the discrete states on the lifetimes of the resonances is *not* negligible.

We also performed calculations with the elastic proton decay channel instead of the elastic neutron decay channel. Qualitatively these pictures show the same phenomena as the pictures for the neutron channel presented above. Also in the case of a proton decay channel, a discrete state with large $\tilde{\Gamma}_R(E_{lab})$ can trap all the resonances.

4 The cross section

Generally, the number of short-lived resonances, created by the trapping effect, is equal to the number of open deacy channels [3] (see eq. (10). In some cases considered in this paper we observed, however, trapping for *all* resonance states. In these cases, no short-lived resonances are formed at large α. Instead, the $\tilde{\Gamma}_R(E_{lab} > 0)$ of one of the discrete states raises up

to a large value with increasing coupling strength α (the calculations are performed at a positive energy E_{lab} of the system).

This result raises the question of the physical meaning of the $\tilde{\Gamma}_R(E_{lab} > 0)$ of the discrete states. Is it possible to observe any hints of them?

A value of physical relevance is the total cross section σ^{tot}. Since the shape of σ^{tot} is an interference picture it is, generally, complicated even in the case of only a few resonances [22]. In order to study the behaviour of a system with only trapped resonances, we considered therefore first a simple example with only one discrete state and one resonance.

Fig. 4 shows the total cross section calculated for a fixed coupling strength ($\alpha = 2$) for the case with one open neutron channel and one and two states, respectively. In Fig. 4.a, the total cross section (full line) with one resonance and the direct reaction part (dashed line) are shown. Because of the neighbourhood of the elastic threshold the resonance shape is non-symmetric with a comparably long tail to larger energies. The minimum at $E_{lab} \rightarrow 0$ arises from interferences between the resonance and the direct reaction part.

In the calculation shown in Fig. 4.b, only one discrete state is considered which is placed very close to the energy of the threshold. In spite of the fact that there are no resonances, the total cross section (full line) shows a stronger increase for $E_{lab} \rightarrow 0$ compared to the direct part (dashed line). This increase can be considered as due to the tail from the state below the threshold. A similar phenomenon is known from the study of resonances around inelastic thresholds [26, 7, 10]. In those papers a cusp in the cross section appears, which is caused by the strong increase of the width of a resonance around the inelastic threshold. In the case considered by us, the widths of the resonances increase from zero at $E_{lab} \leq 0$ to their values $\tilde{\Gamma}_R \approx const$ at larger energies E_{lab}.

In Fig. 4.c the cross section for one discrete state and one resonance is drawn. Also, the direct part is shown (dashed) and the result of Fig. 4.b (dash-dotted). Comparing Fig. 4.c with Figs. 4.a and 4.b one sees the following: σ^{tot} at the resonance is smaller than in Fig. 4.a (note the different scales of σ^{tot} in Figs. 4.a and 4.c) while the cross section for $E_{lab} \rightarrow 0$ shows the tail of a broader state than in Fig. 4.b. Additionally the shape of the resonance resembles a typical interference picture of overlapping resonances in spite of the fact that this calculation is performed with only *one* resonance.

Fig. 4 demonstrates clearly, that discrete states states can influence directly the cross section and also that discrete states are able to trap reso-

nances. The latter result can be seen in the fact that the resonance part of the cross section and the width of the resonance are reduced.

To consider a more realistic case we arranged one bound state directly situated below the elastic threshold together with 186 resonances which can decay via the elastic neutron channel. The complex eigenvalues of the relevant part of the spectrum, calculated for $\alpha = 2.5$ and $E_{lab} = 4MeV$, are shown in Fig. 5.a. (In the spectrum a gap in the energy range just above the threshold is created by removing three shell model states from the direct proximity of the threshold). Also in this case, the eigenvalue of the discrete state (indicated by an arrow) carries the largest imaginary part. All the 186 resonances are trapped.

The total cross section σ^{tot} calculated for this arrangement (Fig. 5.a) is drawn in Fig. 5.b.. (full line) and compared with the direct reaction part (dashed curve). To the left in Fig. 5.b, the cross section close to the elastic threshold is drawn in a 12 times larger ordinate-scale. The abscisse is common to both parts of the plot. As a result σ^{tot} increases much stronger for energies $E_{lab} \rightarrow 0$ than the direct reaction part. The imaginary part of the eigenvalue of the discrete state, calculated at a positive energy, achieves a physical meaning in the cusp structure of the cross section at the elastic threshold. At positive energies, the discrete state acts as a resonance the width of which corresponds to the value $\tilde{\Gamma}_R(E_{lab})$. Fig. 5.b also shows that the line shape of the resonances resembles the picture of interfering resonances.

We also calculated σ^{tot} for the case of one open proton decay channel, and the spectrum partly discrete and partly resonant. We used 190 states and $\alpha = 3.5$. The imaginary part of one of the eigenvalues with the real part of the eigenvalue negative (calculated at $E_{lab} > 0$) is much larger than that of all the other eigenvalues.

Due to the Coulomb repulsion the cross section goes to zero as $E_{lab} \rightarrow 0$ (Fig. 6). This destroys the effect discussed above (Fig. 5) for small energies. Nevertheless a broad structure different from the direct reaction part can be seen for energies between about $1MeV$ and $5MeV$. This difference indicates that the discrete state influences the cross section also in the presence of the Coulomb forces.

5 Conclusions

We investigated in this paper the properties of an ensemble of dense-lying states close to the elasic threshold. As a result, a situation may occur in which *all* the resonances of the ensemble are trapped. The trapping is caused, in such a case, by a discrete state with a large imaginary part $\tilde{\Gamma}_R$ of the eigenvalue of the effective Hamiltonian $H^{eff}_{QQ}(E)$ when calculated at positive energies E_{lab}.

It is also shown that a discrete state with a large $\tilde{\Gamma}_R(E_{lab} > 0)$ which is situated sufficiently close to the threshold can essentially influence the cross section. In the case of a neutron channel we can see a tail from the discrete state. This tail can be understood as an extreme case of a cusp. In the case of a proton channel the effect is destroyed by the Coulomb barrier for small energies.

Finally we briefly state some possible conclusions from our investigations which may be of interest for the neutron resonances. Due to the high level density of the neutron resonances we have reasons to expect the trapping effect to be one of the causes of their small widths. The point of this paper is that the proximity to the threshold does not make this proposal less plausible. It is even possible that resonances near the elastic threshold are trapped by a discrete state.

Further, the results obtained in the present paper give some justification for 'fictive' single-particle states and 'fictive' bound states. Such states are sometimes introduced in order to describe the properties of the neutron resonances.

In a forthcoming paper we will further analyse the possibility of interpreting the neutron resonances as trapped states. Of special interest is the mixing of their wavefunctions.

Acknowledgements

Valuable discussions with F. Dittes, T. Gorin and J. Okołowicz are greatly acknowledged. The investigations are supported by the Deutsche Forschungsgemeinschaft (DFG 922/1).

Figure 1

The complex eigenvalues of the effective Hamiltonian for α varied from 0.05 to 8 in steps of 0.05 (1.a) and $\tilde{\Gamma}_R$ versus α (1.b). The calculations are performed with only the elastic neutron channel, $E_{lab} = 29MeV$, $Q = 20.7MeV$, 190 states in O^{16} with 2p-2h excitations and $J^\pi = 1^-$. The ordinate scale is logarithmic.

Figure 2

The complex eigenvalues of the effective Hamiltonian for the same states as in Fig. 1 but with shell model energies decreased by $25MeV$, $E_{lab} = 4MeV$ and one open neutron channel.

Figure 3

The complex eigenvalues of the same states as in fig. 2, but with a gap in the spectrum around the elastic threshold. The states with negative shell model energy are shifted down in energy by $3MeV$ and the states with positive energy are shifted up by $5MeV$.

Figure 4

Cross section calculated for one open neutron channel and one resonance state (full line in 4.a), no resonance state but one discrete state (full line in 4.b), one discrete state and one resonance state (full line in 4.c) and only one discrete state (dashed-dotted line in 4.c). The dashed lines show the direct reation part of the cross section.

Figure 5

The complex eigenvalues of the effective Hamiltonian for the same states as in Fig. 1, but with shell model energies decreased by $12.7MeV$ and three shell model states removed from the proximity of the threshold ($-1MeV \leq \tilde{E}_R \leq 10MeV$). $E_{lab} = 4MeV$, only one neutron channel is open and $\alpha = 2.5$ (5.a). The discrete state is marked with an arrow. The cross section for this arrangement is shown in 5.b. In the left part of the plot, the cross section is shown in 12 times larger ordinate-scale than in the right part. The abscisse is common to both parts of the plot. The full lines are the total cross section and the dashed lines are the direct reaction part.

Figure 6

Cross section calculated for 190 states, one open proton channel and $\alpha = 3.5$. The spectrum is partly discrete and partly resonant similar to that in Fig. 2. The full lines are the total cross section and the dashed lines are the direct reaction part.

References

[1] P. Kleinwächter and I. Rotter, Phys. Rev. C 32, 1742 (1985)

[2] H. Friedrich and D. Wintgen, Phys. Rev. A 32, 3231 (1985)

[3] V.V. Sokolov and V.G. Zelevinsky, Phys. Lett. B 202, 10 (1988); Nucl. Phys. A 504, 562 (1989)

[4] V.B. Pavlov-Verevkin, Phys. Lett. A 129, 168 (1988); F. Remacle, M. Munster, V.B. Pavlov-Verevkin and M. Desouter-Lecomte, Phys. Lett. A 145, 265 (1990)

[5] F.M. Dittes, W. Cassing and I. Rotter, Z. Phys. A 337, 243 (1990)

[6] P. von Brentano, Phys. Lett. B 238, 1 (1990); B 246, 320 (1990); Nucl. Phys. A 550, 143 (1992)

[7] I. Rotter, Rep. Prog. Phys. 54, 635 (1991) and references therein

[8] F.M. Dittes, I. Rotter and T.H. Seligman, Phys. Lett. A 158, 14 (1991)

[9] F.M. Dittes, H.L. Harney and I. Rotter, Phys. Lett. A 153, 451 (1991)

[10] V.V. Sokolov and V.G. Zelevinsky, Ann. Phys. (N. Y.) 216, 323 (1992) and references therein

[11] F. Haake, F. Izrailev, N. Lehmann, D. Saher and H.J. Sommers, Z. Phys. B 88, 359 (1992)

[12] R.D. Herzberg, P. von Brentano and I. Rotter, Nucl. Phys. A 556, 107 (1993)

[13] W. Iskra, I. Rotter and F.-M. Dittes, Phys. Rev. C 47, 1086 (1993)

[14] A. Mondragon and E. Hernandez, J. Phys. A 26, 5595 (1993); Phys. Lett. B 326, 1 (1994)

[15] K. Someda, H. Nakamura and F.H. Mies, Chem. Phys. 187, 195 (1994) (1994)

[16] A. Bürgers and D. Wintgen, J. Phys. B 27, L131 (1994)

[17] W. Iskra, M. Müller and I. Rotter, J. Phys. G 19, 2045 (1993); G 20, 775 (1994)

[18] F. M. Izrailev, D. Saher and V. V. Sokolov, Phys. Rev. E 49, 130 (1994)

[19] W. Iskra, M. Müller and I. Rotter, Phys. Rev. C 51, 1842 (1995)

[20] E. Sobeslavsky, F.-M. Dittes and I. Rotter, J. Phys. A 28, 2963 (1995)

[21] M. Desouter-Lecomte, J. Liévin and V. Brems, J. Chem. Phys. 103, 4524 (1995)

[22] M. Müller, F.-M. Dittes, W. Iskra and I. Rotter, Preprint FZR-70 (Rossendorf 1995); Phys. Rev. E, December 1995

[23] C. Mahaux and H.A. Weidenmüller, *Shell Model Approach to Nuclear Reactions*, Amsterdam: North-Holland, 1969

[24] A. Bohr and B. Mottelson, R 1975 *Nuclear Reactions* (London: Benjamin)

[25] H.W. Barz, I. Rotter and J. Höhn, Nucl. Phys. A 275, 111 (1977)

[26] I. Rotter, H.W. Barz, and J. Höhn, Nucl. Phys. A 297, 237 (1978)

1.a

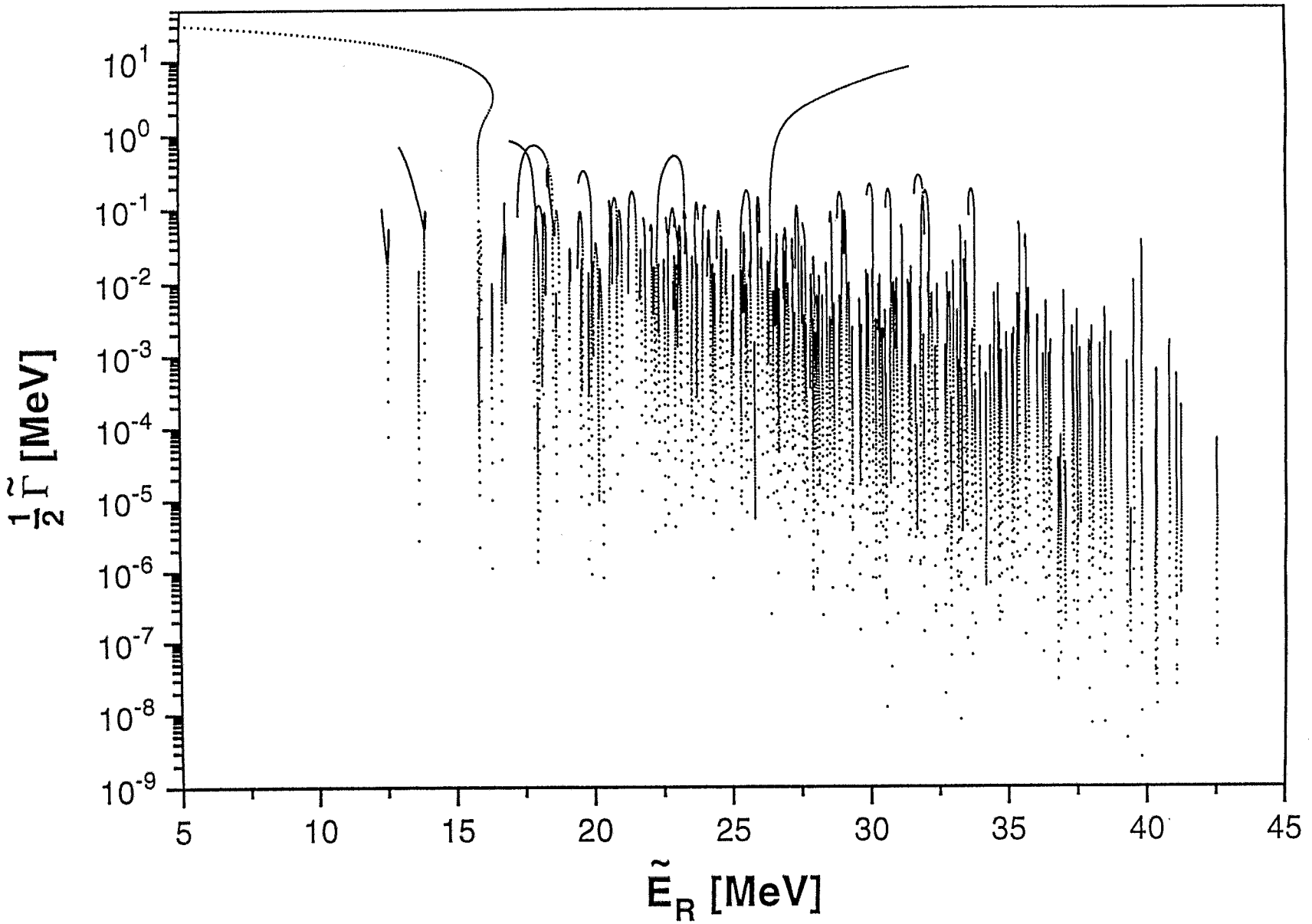
10^{1}
10^{0}
10^{-1}
10^{-2}
10^{-3}
10^{-4}
10^{-5}
10^{-6}
10^{-7}
10^{-8}
10^{-9}
$\frac{1}{2}\tilde{\Gamma}$ [MeV]
5
10
15
20
25
30
35
40
45
$\tilde{E}_R$ [MeV]

1.b

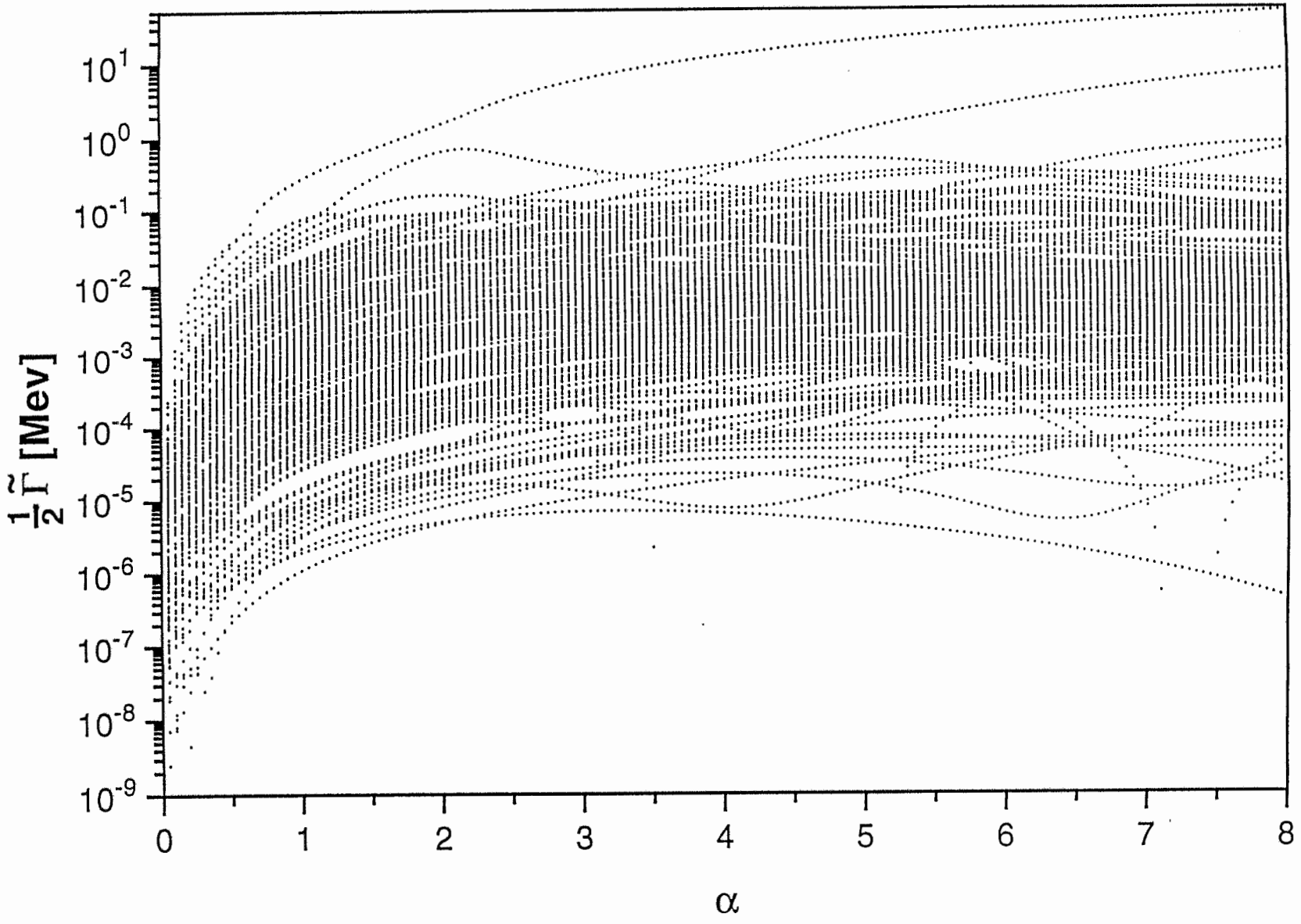
10^{1}
10^{0}
10^{-1}
10^{-2}
10^{-3}
10^{-4}
10^{-5}
10^{-6}
10^{-7}
10^{-8}
10^{-9}
$\frac{1}{2}\tilde{\Gamma}$ [Mev]
0
1
2
3
4
5
6
7
8
α

2

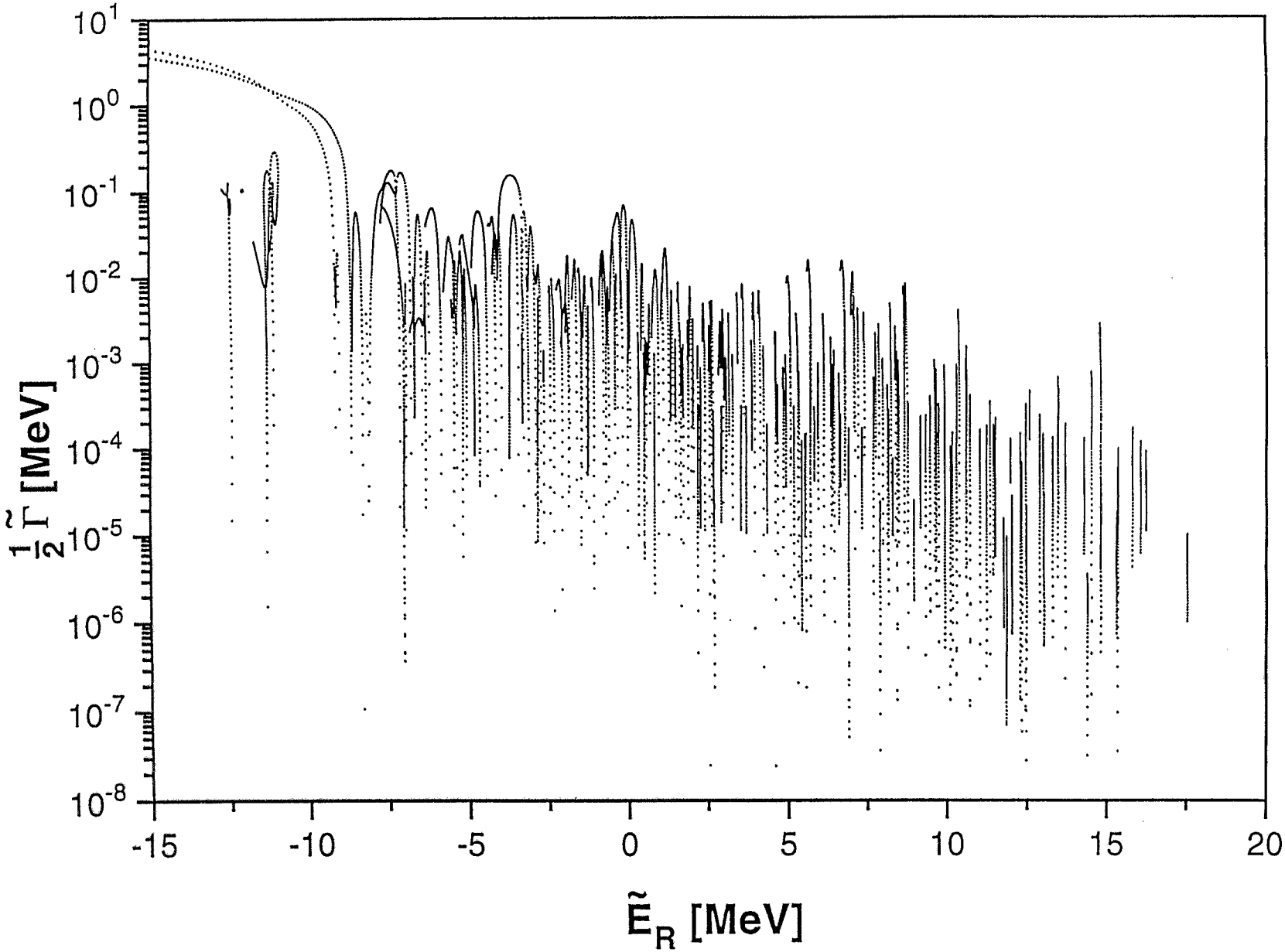
10^{1}
10^{0}
10^{-1}
10^{-2}
10^{-3}
10^{-4}
10^{-5}
10^{-6}
10^{-7}
10^{-8}
$\frac{1}{2}\tilde{\Gamma}$ [MeV]
-15
-10
-5
0
5
10
15
20
$\tilde{E}_R$ [MeV]

3

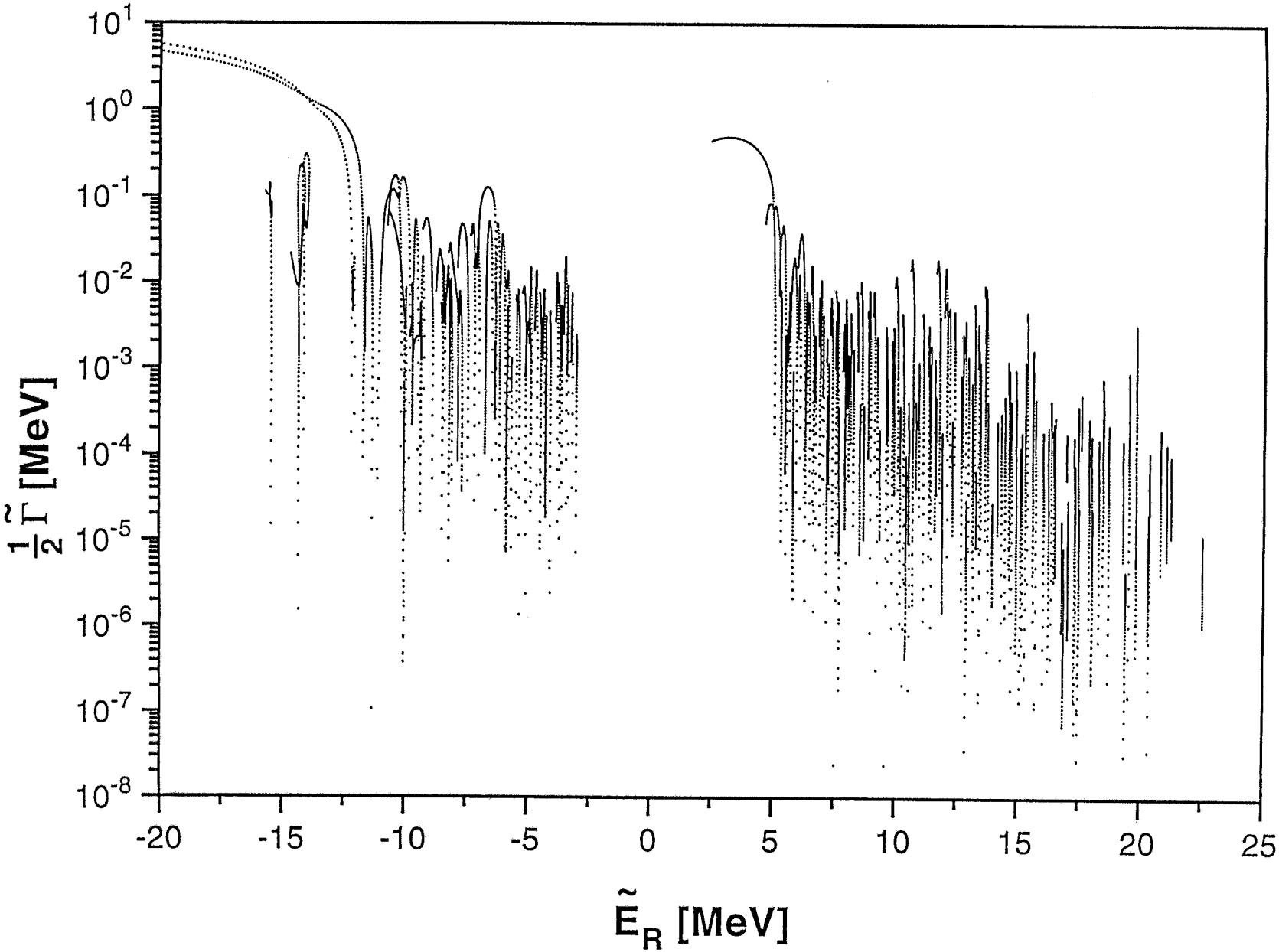
10^{1}
10^{0}
10^{-1}
10^{-2}
10^{-3}
10^{-4}
10^{-5}
10^{-6}
10^{-7}
10^{-8}
$\frac{1}{2}\tilde{\Gamma}$ [MeV]
-20
-15
-10
-5
0
5
10
15
20
25
$\tilde{E}_R$ [MeV]

4.a

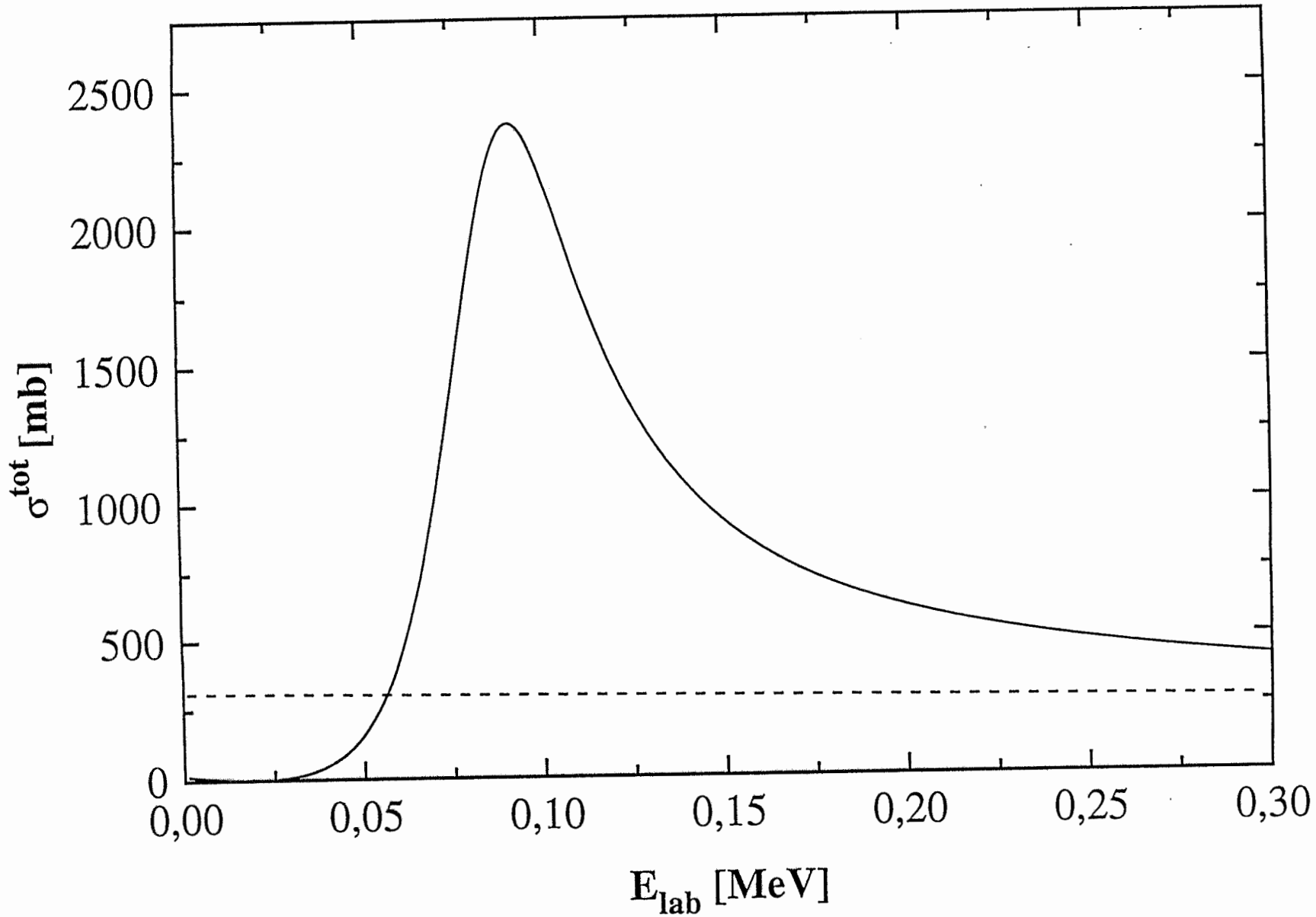
2500
2000
1500
1000
500
0
σ^{tot} [mb]
0,00
0,05
0,10
0,15
0,20
0,25
0,30
E_{lab} [MeV]

4.b

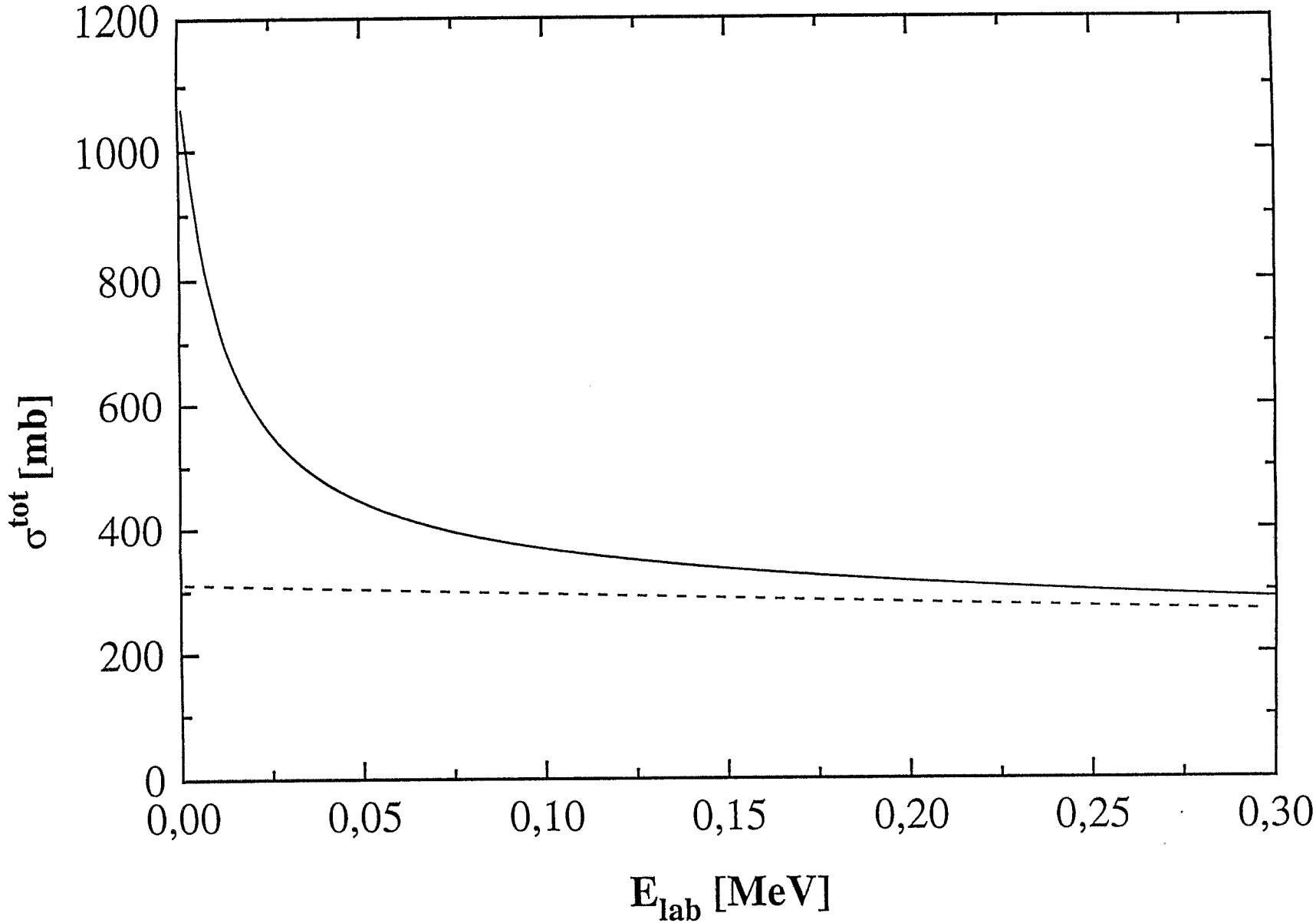
1200
1000
800
600
400
200
0
σ^{tot} [mb]
0,00
0,05
0,10
0,15
0,20
0,25
0,30
E_{lab} [MeV]

4.c

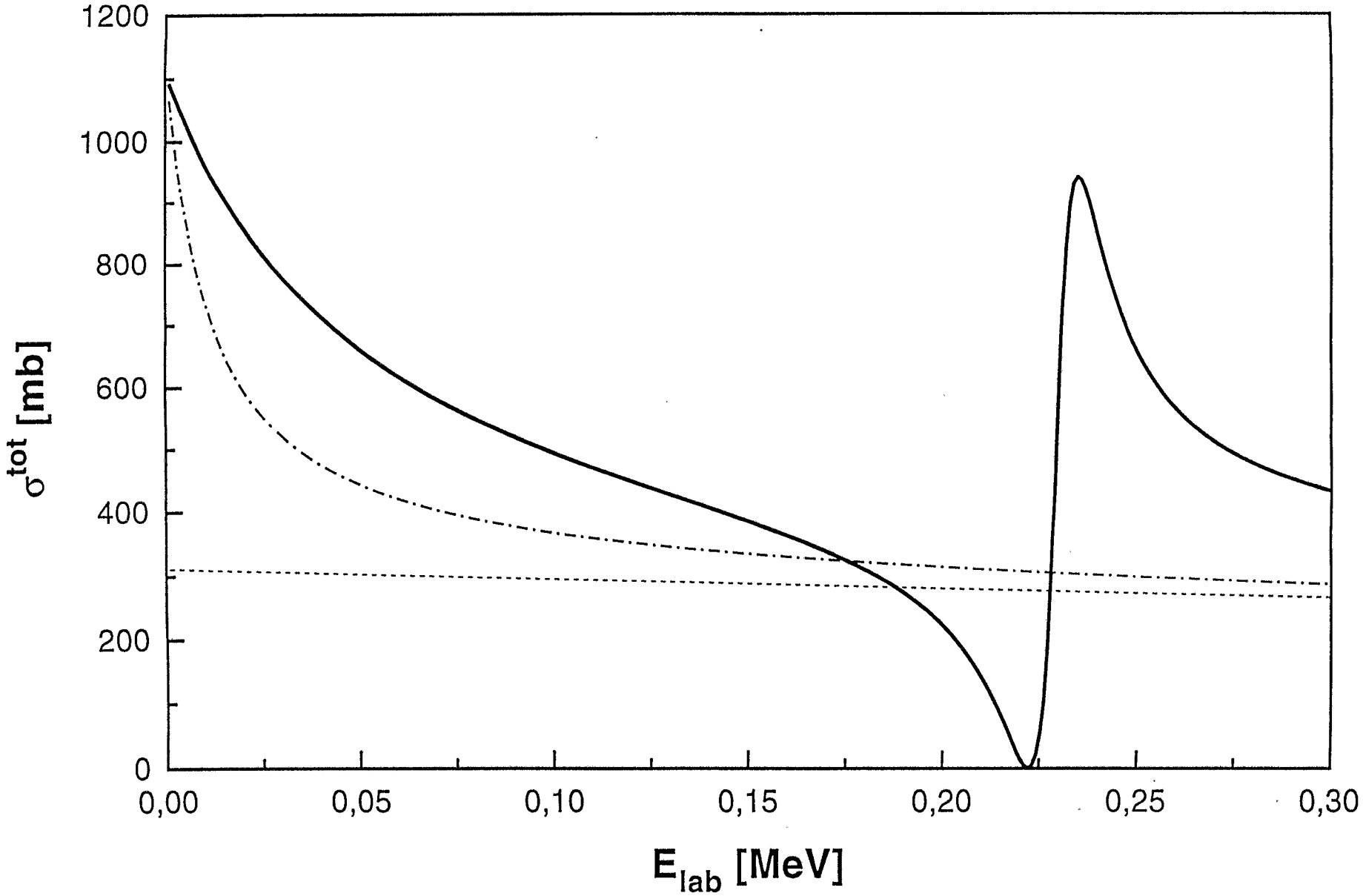
1200
1000
800
600
400
200
0
σ^{tot} [mb]
0,00
0,05
0,10
0,15
0,20
0,25
0,30
E_{lab} [MeV]

5.a

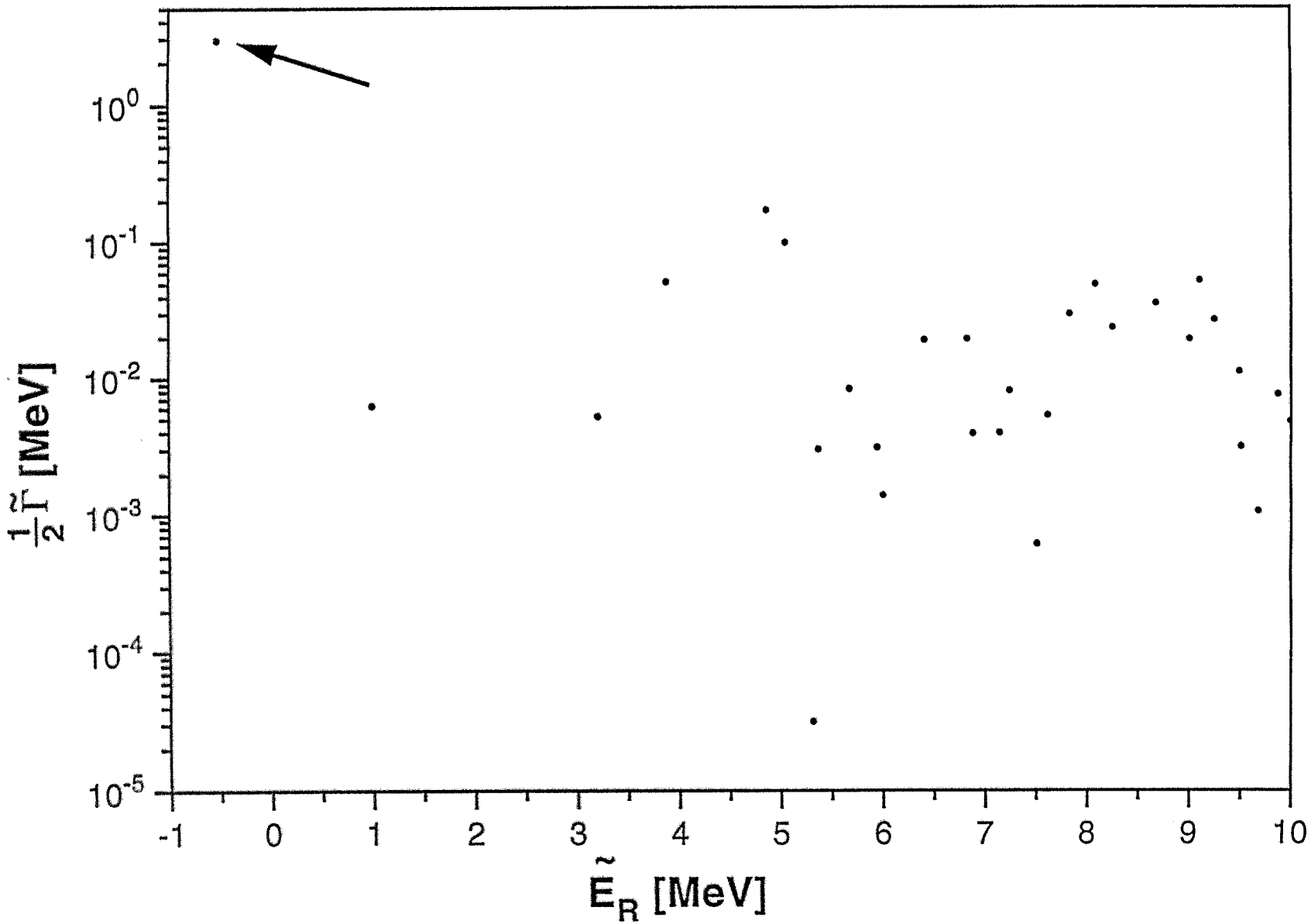
10^0
10^{-1}
10^{-2}
10^{-3}
10^{-4}
10^{-5}
$\frac{1}{2}\tilde{\Gamma}$ [MeV]
-1
0
1
2
3
4
5
6
7
8
9
10
$\tilde{E}_R$ [MeV]

5.b

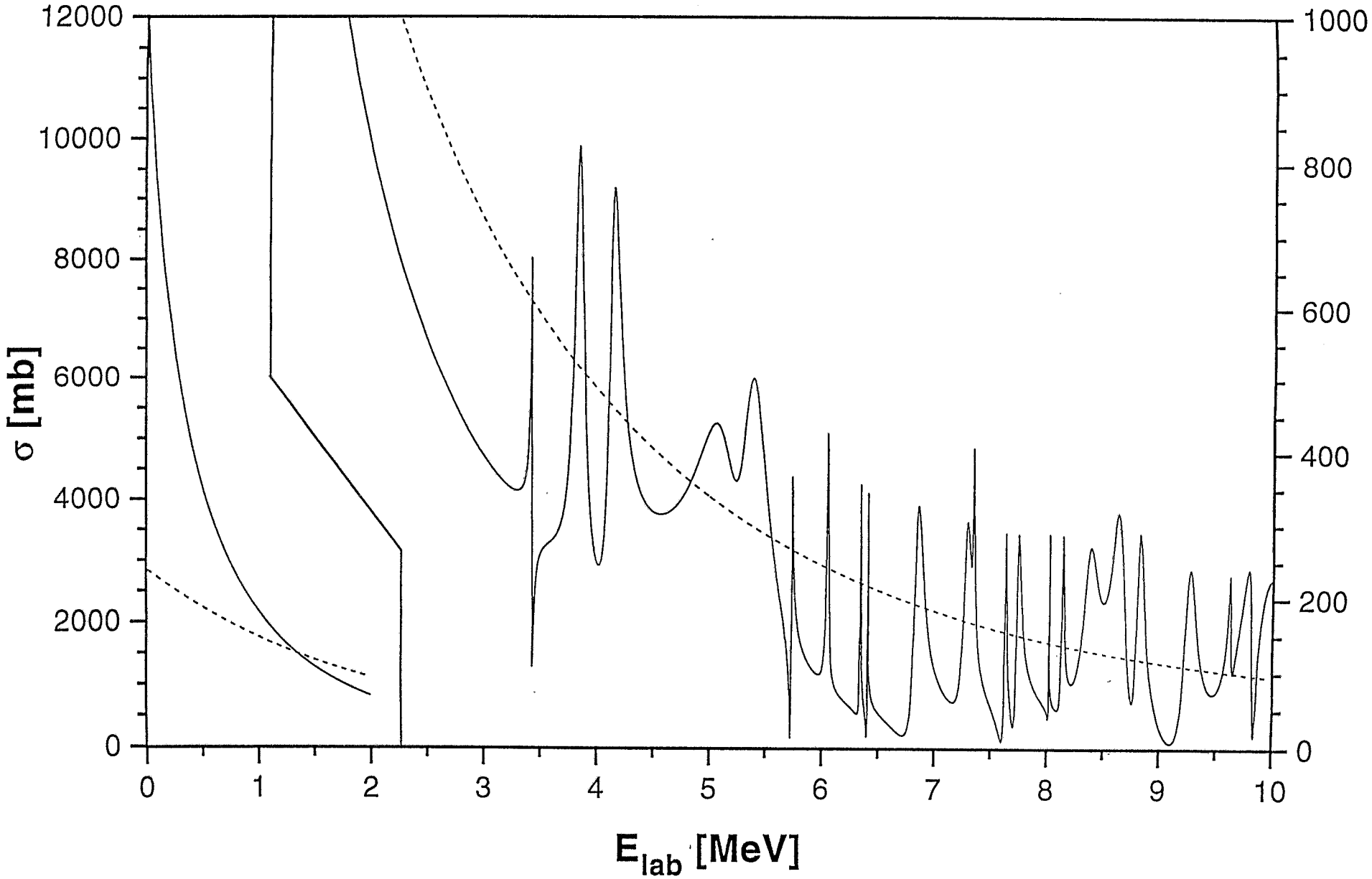
12000
10000
8000
6000
4000
2000
0
σ [mb]
1000
800
600
400
200
0
0
1
2
3
4
5
6
7
8
9
10
E_lab [MeV]

6

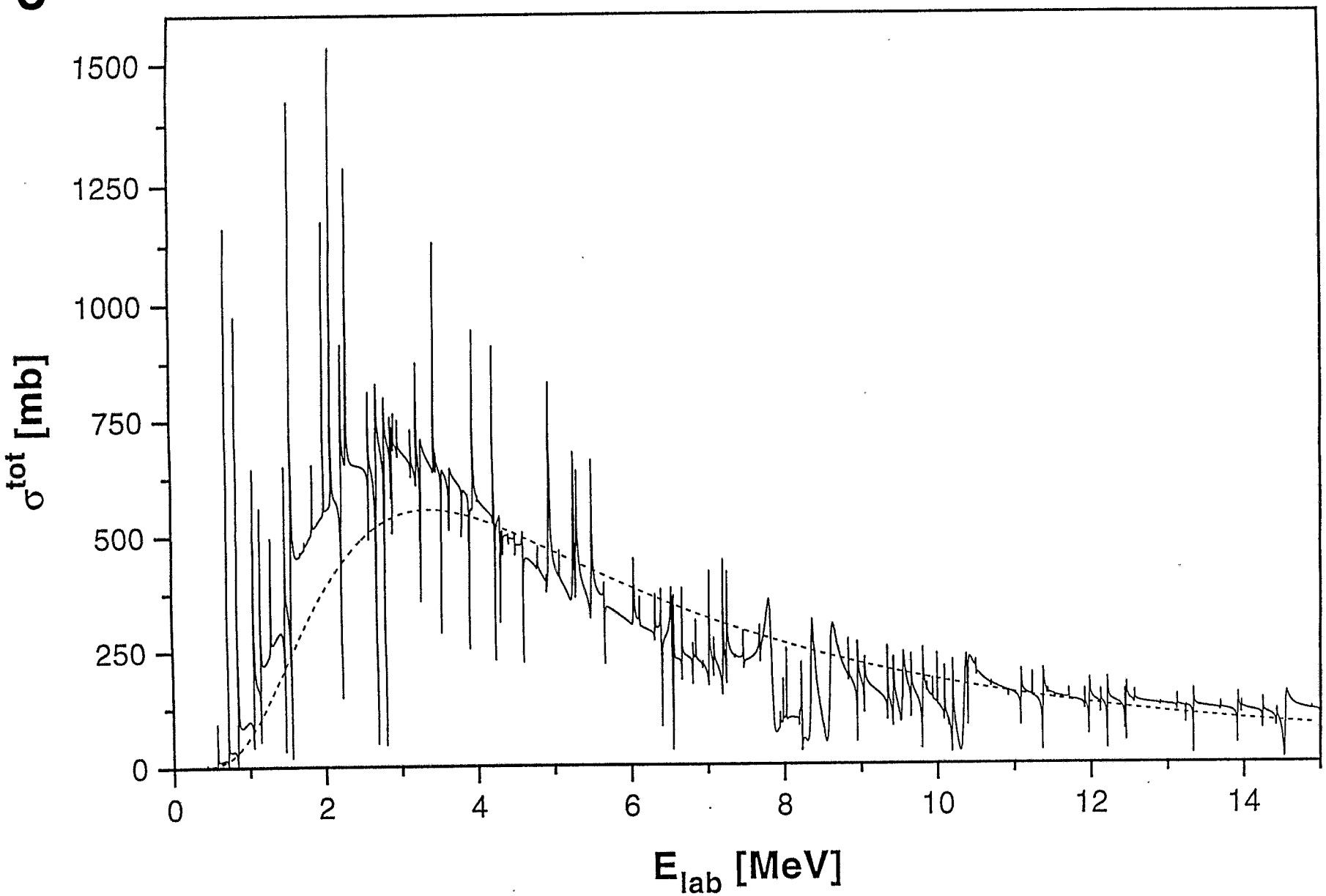
1500
1250
1000
750
500
250
0
σ^{tot} [mb]
0
2
4
6
8
10
12
14
E_{lab} [MeV]